NASA TECHNICAL MEMORANDUM

NASA TM X-3299

NASA TM X-3299

SILICON NITRIDE-ALUMINUM OXIDE SOLID SOLUTION (SiAION) FORMATION AND DENSIFICATION BY PRESSURE SINTERING

Hun C. Yeh, William A. Sanders, and Jere L. Fiyalko

Lewis Research Center
Cleveland, Ohio 44135

NATIONAL AERONAUTICS AND SPACE ADMINISTRATION • WASHINGTON, D. C. • OCTOBER 1975

1. Report No.	2. Government Accession No.	3. Recipient's Catalog No.
NASA TM X-3299		

4. Title and Subtitle	5. Report Date
SILICON NITRIDE - ALUMINUM OXIDE SOLID SOLUTION (SiAlON) FORMATION AND DENSIFICATION BY PRESSURE SINTERING	October 1975
	6. Performing Organization Code
7. Author(s) Hun C. Yeh, Cleveland State University, Cleveland, Ohio; and William A. Sanders and Jere L. Fiyalko, both of Lewis Research Center	8. Performing Organization Report No. E-8317
	10. Work Unit No. 505-01
9. Performing Organization Name and Address Lewis Research Center National Aeronautics and Space Administration Cleveland, Ohio 44135	11. Contract or Grant No.
	13. Type of Report and Period Covered Technical Memorandum
12. Sponsoring Agency Name and Address National Aeronautics and Space Administration Washington, D. C. 20546	14. Sponsoring Agency Code

15. Supplementary Notes

16. Abstract

Stirred-ball-mill-blended Si_3N_4 and Al_2O_3 powders were pressure sintered in order to investigate the mechanism of solid-solution formation and densification in the Si_3N_4-Al_2O_3 system. Powder blends with Si_3N_4:Al_2O_3 mole ratios of 4:1, 3:2, and 2:3 were pressure sintered at 27.6-MN/m^2 (4000-psi) pressure at temperatures to 1700^o C (3090^o F). The compaction behavior of the powder blends during pressure sintering was determined by observing the density of the powder compact (ram travel) as a function of temperature and time starting from room temperature. This information, combined with the results of X-ray diffraction and metallographic analyses regarding solutioning and phase transformation phenomena in the Si_3N_4-Al_2O_3 system, was used to describe the densification behavior.

17. Key Words (Suggested by Author(s))	18. Distribution Statement
Silicon nitride - aluminum oxide Ceramics Refractory compounds Pressure sintering	Unclassified - unlimited STAR Category 27 (rev.)

19. Security Classif. (of this report)	20. Security Classif. (of this page)	21. No. of Pages	22. Price*
Unclassified	Unclassified	28	$3.75

* For sale by the National Technical Information Service, Springfield, Virginia 22161

SILICON NITRIDE - ALUMINUM OXIDE SOLID SOLUTION (SiAlON) FORMATION AND DENSIFICATION BY PRESSURE SINTERING

by Hun C. Yeh*, William A. Sanders, and Jere L. Fiyalko

Lewis Research Center

SUMMARY

In this experimental study, precompacted mixtures of silicon nitride (Si_3N_4) and aluminum oxide (Al_2O_3) powders were pressure sintered under vacuum in order to investigate the mechanism of formation and densification in the Si_3N_4-Al_2O_3 system. Intensive mixing and comminution of the fine-particle-size powders was attained by using a stirred-ball mill.

Powder blend compacts of Si_3N_4 plus Al_2O_3 in mole ratios of 4:1, 3:2, and 2:3 were vacuum pressure sintered at temperatures from 1100° to 1700° C (2010° to 3090° F) for as long as 2 hours at a pressure of 27.6 MN/m^2 (4000 psi). Pore-free compacts with only a trace of second phase were obtained at temperatures as low as 1500° C (2730° F) with the 40-mol % Si_3N_4 - 60-mol % Al_2O_3 composition. (All Si_3N_4-Al_2O_3 compositions are in mole percent and will hereinafter be given in the form $40Si_3N_4$-$60Al_2O_3$.)

Ram travel recorded during pressure sintering indicated high densification rates in the temperature range 1400° to 1700° C (2550° to 3090° F) with a maximum at 1500° C (2730° F). Densification rates and end-point densities were correlated with the results of X-ray diffraction and metallographic analyses to characterize the solutioning and phase transformations in the Si_3N_4-Al_2O_3 system.

INTRODUCTION

Silicon nitride (Si_3N_4) in both the pressure-sintered (hot pressed) and reaction-sintered forms offers a great potential for use in hot-flow-path components in gas

---

*Associate Professor of Metallurgy, Cleveland State University, Cleveland, Ohio; Summer Faculty Fellow at the Lewis Research Center in 1974.

turbine engines (refs. 1 to 6). Although the strength properties of Si_3N_4 materials are good, materials of higher strength are desired. For hot-pressed Si_3N_4 (HPSN), high-temperature strength begins to be impaired above approximately 1200° C (2190° F) because of a glassy, silicate, grain boundary phase (ref. 7). This silicate phase is a consequence of an addition of magnesium oxide (MgO) required for obtaining high density. Reaction-sintered Si_3N_4 (RSSN) does not suffer from high-temperature-strength degradation since it is essentially free of any glassy grain boundary phase. But RSSN, by the nature of its fabrication process (nitriding of silicon powder compacts), is at present limited to about 70 percent of theoretical density and is thus not as strong as HPSN. However, the strength of RSSN is insensitive to increasing temperature, and indications are that 75-percent-dense RSSN is actually stronger than HPSN above approximately 1400° C (2550° F) (ref. 8). It follows that a material should have the high density and high strength of HPSN with the strength maintenance exhibited by RSSN.

In developing a material for quantity use, such as for the hot-flow-path components of gas turbine engines, an economical production method is a major consideration. Parts can be more easily fabricated to shape from RSSN than from HPSN. Slip casting or injection molding is used for RSSN parts in comparison to the more expensive hot-pressing procedure, which must be followed by costly diamond grinding of parts. Thus RSSN, although not as strong as HPSN, is considered an attractive material for certain turbine components.

With these considerations in mind, it is understandable that a paper by Jack and Wilson (ref. 9) describing the excellent properties of pressureless-sintered Si_3N_4 base materials of low porosity (viz 7 percent) evoked considerable interest. Jack and Wilson describe a Si_3N_4 material of an expanded beta (β) Si_3N_4 crystallographic form, termed β' (beta prime), which resulted from the solutioning of aluminum oxide (Al_2O_3) into Si_3N_4 during sintering of Si_3N_4-Al_2O_3 powder mixtures. Such sintered bodies (termed "SiAlON ceramics" by Jack and Wilson) were found to have a lower coefficient of thermal expansion than HPSN, which is good from thermal shock considerations. And these sintered bodies did indeed exhibit excellent thermal shock resistance. The sintered SiAlON bodies were also found by Jack (ref. 10) to be more oxidation resistant than HPSN in 1300° C (2370° F), 150-hour oxidation tests. He observed that perhaps the greatest advantage of the SiAlON material over HPSN was its ease of fabrication. And he related this sinterability to the promotion of diffusion by vacant lattice sites. Very recently, Drew and Lewis (ref. 11) have found metallographic evidence for liquid-phase sintering of sintered and hot-pressed Si_3N_4-Al_2O_3 powder mixtures.

The interest generated in SiAlON materials by the Jack and Wilson paper (ref. 9) has resulted in efforts by several research groups to consolidate SiAlON bodies (refs. 12 to 14). Arrol (ref. 12) confirms the superior oxidation resistance of SiAlON over HPSN that is reported in reference 9. But he indicates that impurities are responsible for the

sintering ease of certain SiAlON's and that higher-density (purer) SiAlON's are not so easily sintered. As reported in reference 9, SiAlON's were found to be more easily hot pressed than HPSN; some SiAlON bodies exhibited superior creep resistance to HPSN at 1225° C (2240° F) and 69-MN/m^2 (10 000-psi) load. Lange (ref. 13) also found it difficult to obtain high-density SiAlON bodies by sintering but did obtain high-density SiAlON bodies by hot pressing. Contrary to Jack and Wilson (ref. 9), Lange found that his hot-pressed SiAlON of the same nominal composition as that of Jack and Wilson had a greater coefficient of thermal expansion than HPSN. Likewise, Crandall, Hed, and Shipley (ref. 14) found it difficult to sinter SiAlON, achieving at best only 80 percent of theoretical density. However, they did obtain pore-free compacts by hot pressing.

From this brief summary of the results obtained by Arrol (ref. 12), Lange (ref. 13), and Crandall (ref. 14), the high sinterability of SiAlON reported by Jack and Wilson (ref. 9) is seen to be problematical. In references 12 to 14, it was commonly concluded that the type and amount of second phases (some possibly liquid) occurring with the SiAlON (Si_3N_4-Al_2O_3 solid solution) major phase are very important, as are starting material purities and consolidation process conditions.

The study reported herein was conducted to provide some further insight into the mechanism of the formation and densification of SiAlON material. In this study, intensive stirred-ball-mill blending of starting powders assured excellent mixing and contact of Si_3N_4 and Al_2O_3 powders. In order to characterize the kinetics of reaction and densification, powder blends of various Si_3N_4:Al_2O_3 mole ratios were pressure sintered in vacuum at temperatures from 1100° to 1700° C (2010° to 3090° F). Press ram travel due to the application of a constant pressure (a measure of powder compaction) was recorded during heating and at equilibrium temperature. Powder compaction rates and end-point densities were correlated with X-ray diffraction and metallographic analyses to describe SiAlON formation and densification as a function of temperature and Si_3N_4:Al_2O_3 mole ratio.

MATERIALS

The starting materials were Plessey Co., Ltd., α-Si_3N_4 and Cabot Corp. AlON γ-Al_2O_3 powders. The Si_3N_4 powder was reported by the supplier to be 94 percent α-phase plus 6 percent β-phase. It was also determined at the NASA Lewis Research Center to contain 0.92 wt % oxygen and 0.22 wt % carbon by inert-gas fusion and induction heating - chromatographic finishing, respectively. The Si_3N_4 powder contained 50 to 260 ppm calcium, 800 to 1200 ppm aluminum, and 300 to 500 ppm iron as determined by semiquantitative spectrographic analyses also performed at Lewis. The Al_2O_3 powder was reported by the supplier to be essentially 100 percent γ-phase and to

have a metal impurity content of less than 0.1 percent. The morphology and size ranges of the as-received powders were characterized by transmission electron microscopy (TEM). Plessey α-Si_3N_4 consists of fibrous and flake-like crystallites (fig. 1(a)). The flakes range in size from 0.02 to 1.0 micrometer and the fibers from 0.04 to 0.3 micrometer with a wide variation in length. The γ-Al_2O_3 powder particles are round in shape (fig. 1(b)) and are positively charged (according to the supplier). Particle size ranges from 0.005 to 0.09 micrometer and is predominantly in the 0.01- to 0.02-micrometer range.

APPARATUS AND PROCEDURE

Each powder mixture (50-g batch weight) with the desired Si_3N_4:Al_2O_3 mole ratio was blended and ground at a controlled speed in a nickel stirred-ball mill with 3-millimeter-diameter steel grinding balls (ball- to powder-weight ratio of 44:1) and a liquid solution of 3 percent alcohol in heptane. In order to control the amount of iron pickup to a relatively constant level, 0.4 to 0.8 wt %, the blending time was varied between 1 to 2 hours, depending on the Si_3N_4:Al_2O_3 mole ratio. It had been found in a preliminary experiment that for a given blending time the amount of iron pickup increased with the concentration of Si_3N_4 in the powder mixture. After blending, the powder mixture was dried in air and then in vacuum for at least 24 hours. Based on a 100-mol %-Si_3N_4 blending, oxygen pickup for the Si_3N_4-Al_2O_3 mixtures is estimated to range from about 1.6- to 2.5-wt % oxygen. A transmission electron microscope characterization of the $40Si_3N_4$-$60Al_2O_3$ mixture after stirred-ball-mill blending is shown in figure 2. The very fine Al_2O_3 particles remain unchanged, but the rod-like Si_3N_4 particles have been broken. The large particles are probably agglomerates of Si_3N_4 particles with adhering Al_2O_3 particles.

A schematic of the vacuum induction furnace used for pressure sintering is shown in figure 3. The furnace, which is induction heated with a graphite susceptor, was run under a vacuum of 4 to 0.006 N/m^2. A port in the water-cooled manifold that is welded to the top plate connects the vacuum system to the furnace. The graphite susceptor, 15.6 centimeters ($6\frac{1}{8}$ in.) in diameter and 40.6 centimeters (16 in.) long, and the carbon susceptor extension rest on the water-cooled bottom plate. The susceptor is positioned inside a 25.4-centimeter- (10-in.-) diameter, 81.3-centimeter- (32-in.-) long, fused-quartz tube. A water-cooled induction coil, powered by a 9600-hertz, 50-kilowatt motor-generator, is wrapped around the quartz tube. Annular grooves with silicone rubber gaskets are located in the water-cooled top and bottom plates. These grooves secure the quartz tube and tightly seal the vacuum chamber. The annular space between the susceptor assembly and the quartz tube is filled with carbon black insulation.

A graphite cloth backed by a segmented graphite ring prevents the carbon black insulation from being blown out during evacuation. Four thick tie rods between the top and bottom plates aline the furnace and ensure rigid assembly. The graphite die body rests on a carbon block which clears the susceptor by 0.16 centimeter (1/16 in.). The carbon block rests on the water-cooled base. Above the die are two carbon radiation shields.

The rectangular die opening dimensions are 6.35 centimeters by 1.27 centimeters (2.5 in. by 0.5 in.). Approximately 48 grams of powder were packed in the die, which was coated with boron nitride. The dies packed with powder were first cold pressed by using a hydraulic hand press with 13.8 MN/m^2 (2000-psi) pressure. The die was then loaded into the hot press and 27.6-MN/m^2 (4000-psi) pressure was applied on the powder compact under vacuum. The 27.6-MN/m^2 (4000-psi) pressure was held during both the heating and temperature holding periods. Pressure was completely removed at the onset of cooling.

The sample (powder compact) temperature was measured by a thermocouple placed in a hole in the center of the die body, with the thermocouple hot junction 0.5 centimeter (0.20 in.) from the sample. Temperatures were also monitored with an optical pyrometer by sighting the top of the die through a glass prism mounted on the furnace cover. Temperatures could be generally maintained within 10° C ($\pm 18^{\circ}$ F) of the desired holding temperature by controlling the power supply setting.

One of the main objectives of this study was to examine the compacting behavior of the powder compact during both the heating and temperature holding periods of a pressure sintering run. This was accomplished by monitoring the ram travel shown on a dial gage mounted on the ram with reference to the top of the press. Thus, ram travel, temperature, and time-elapsed data starting from the moment when furnace power was turned on were recorded every 5 minutes during each pressure sintering run.

In order to make meaningful analyses on ram travel - temperature - time data, a fixed heating schedule was followed for all pressure sintering runs in this study. It was accomplished by setting the furnace power input at a certain high rating and then letting the temperature rise naturally. The power input was subsequently reduced to a lower level when the sample temperature (temperature at the center of the die) approached the desired holding temperature. Temperature control by following this procedure was quite reproducible. Figure 4 shows a typical thermal history for a pressure sintering run to 1700° C (3090° F) with a hold at this temperature. For other 1700° C (3090° F) runs in this study, the maximum temperature deviation from this curve was generally $\pm 10^{\circ}$ C ($\pm 18^{\circ}$ F). The same heating schedule was used for all pressure sintering runs.

In order to provide a common base for comparing the compaction behavior among pressure sintering runs, ram travel data from each run were subsequently converted to the transient relative density $\rho_r(T, t)$ of the sample at the corresponding transient tem-

perature T and elapsed time t. This conversion was accomplished by the procedures outlined in the following paragraph.

The transient relative density of a sample of a given composition is defined as

$$\rho_r(T, t) = \frac{\rho(T, t)}{\rho_m} \times 100 \tag{1}$$

where $\rho(T, t)$ is the calculated transient density of the sample based on the ram travel datum at the transient temperature T and the elapsed time t and ρ_m is a measured density. This density ρ_m was obtained from a sample having the same composition as the one under investigation but pressure sintered at the most severe conditions used in this study (2 hr at 1700° C (3090° F) and 27.6 MN/m^2 (4000 psi)). These conditions rendered pore-free microstructures for all three compositions chosen for investigation in this study. Measured densities for these pore-free bodies are listed in table I for the respective compositions. Furthermore, both $\rho(T, t)$ and ρ_m can be expressed in terms of sample weight and sample dimensions:

$$\rho(T, t) = \frac{W}{AxH_i} \tag{2}$$

$$\rho_m = \frac{W}{AxH_f} \tag{3}$$

where W is the sample weight, A the cross-sectional area of the sample as defined by the die opening, H_i the transient thickness of the sample, and H_f the measured thickness (at room temperature) of the sample which had been pressure sintered under the most severe conditions and was pore free. The transient relative density ρ_r is then, by substitution of equations (2) and (3) into equation (1), expressed as

$$\rho_r(T, t) = \frac{H_f}{H_i} \tag{4}$$

RESULTS AND DISCUSSION

Most pressure-sintering (hot pressing) studies on SiAlON materials to date have concerned the end-point density of the sample after a 1- to 2-hour heating at tempera-

tures of 1700° C (3090° F) or higher and pressures of 27.6 MN/m^2 (4000 psi) or higher. The holding temperatures and times used in hot-pressing SiAlON materials have been chosen somewhat arbitrarily based on the experiences gained from hot-pressing studies on Si_3N_4 with MgO as a sintering aid.

In order to provide a better understanding of the compaction behavior of SiAlON materials during pressure sintering, it was decided to investigate the density-temperature-time relation throughout the entire pressure-sintering period at 27.6 MN/m^2 (4000 psi) to 1700° C (3090° F) and also during a 2-hour hold. The density-time-temperature results were correlated with X-ray diffraction analyses and with metallographic analyses of the pressure-sintered samples by scanning electron, light, and transmission electron microscopy. Composition effects on compaction were included in this study by varying the Si_3N_4:Al_2O_3 mole ratio. Therefore, the compaction behavior of the Si_3N_4 and Al_2O_3 powder mixtures can be better understood on the basis of the observed solutioning, phase transformation, microstructure changes, and other physiochemical phenomena.

Relative Density - Transient Temperature Curves

It has been established that Si_3N_4 powders of commercial purity without additives do not densify at all under conventional pressure sintering (hot pressing) conditions (ref. 15). However, when Al_2O_3 powder is mixed with Si_3N_4 powder, full-density bodies (SiAlON) can be obtained by conventional hot-pressing methods (refs. 12 to 14). It is therefore clear that interaction between Al_2O_3 and Si_3N_4 powder particles in a mixed powder sample plays an important role in enhancing densification. This interaction effect was revealed by comparing the relative density - transient temperature (or time) curves of a series of pressure sintering runs under the same conditions but with increasing Al_2O_3 content in the powder mixtures, ranging from 100-percent Si_3N_4 to 100-percent Al_2O_3 powders.

Figure 5 shows the relative density - transient temperature curves for the heating period of pressure sintering runs of 100-percent Si_3N_4 and 100-percent Al_2O_3 as received from the suppliers. No significant densification was observed during the subsequent 2-hour hold at 1700° C (3090° F) in either run. Theoretical densities of Si_3N_4 and Al_2O_3 were used for ρ_m to obtain values of H_f. These H_f values were used to calculate the relative densities ρ_r (by eq. (4)) that were used in plotting the curves of figure 5.

The 100-percent Si_3N_4 curve is essentially horizontal with a slightly negative slope, confirming the nondensifying nature of the material as pointed out previously. The slightly negative slope of the curve is attributed to the thermal expansion of the hot-

pressing system as temperature increased. Distinct densification stages were observed in the relative density - transient temperature curve of the 100-percent Al_2O_3 run. The initial stage in Al_2O_3 densification has been described as resulting from particle sliding, fragmentation, and plastic flow by dislocation motion, with particle sliding being the main contributor to densification (ref. 16). It is not known whether initial densification is enhanced by the transformation of γ-Al_2O_3 to α-Al_2O_3, which occurs between 750° C (1390° F) and 1200° C (2190° F) (ref. 17). But Rice (ref. 18) and Gazza, Barfield, and Preas (ref. 19) report no appreciable differences in minimum hot-pressing parameters required for equivalent densification whether a γ-Al_2O_3 or an α-Al_2O_3 powder is used as the starting material. A stage of inhibited densification for 100-percent Al_2O_3 from approximately 1200° to 1350° C (2190° to 2460° F) is indicated by the plateau region on that curve in figure 5. This behavior, also noted for our Si_3N_4-Al_2O_3 mixture, is similar to that reported by Rice (ref. 18). He found that inhibited densification coincided with heavy outgassing during an interval of the heating period in vacuum hot pressing. Above 1350° C (2460° F) our Al_2O_3 resumed densification, reaching a relative density of 88 percent at 1700° C (3090° F). As noted previously, little additional densification occurred during the subsequent 2-hour holding period. Failure to achieve higher relative density is believed to be due to trapped gaseous impurities, as has been discussed by Rice (ref. 18). These impurities, in quantity, are related to the surface area of the ultrafine γ-Al_2O_3 powder used. At conditions similar to our pressure sintering conditions, Al_2O_3 can be consolidated to close to theoretical density (ref. 20).

Three powder mixtures with decreasing Si_3N_4:Al_2O_3 mole ratios of 4:1, 3:2, and 2:3 (20-, 40-, and 60-mol % Al_2O_3) were chosen for study. These three powder mixtures are listed in table I, along with the composition and density values expressed in three different forms. Calculation of the complete solid solution (β') densities given in table I was based on the SiAlON formula given by Jack and Wilson (ref. 9) and on lattice parameters determined for our pressure-sintered SiAlON compositions. The solubility of Al_2O_3 in Si_3N_4 at 1750° C (3180° F) has been reported to be 67 mol % (ref. 21). Therefore, in order to ensure reasonably complete solutioning, the upper limit of Al_2O_3 content in the mixtures chosen for study was set at 60 mol %.

Relative density - transient temperature curves for pressure sintering runs for the three mixtures, 100-percent Si_3N_4, and 100-percent Al_2O_3 during the heating period (from room temperature to 1700° C (3090° F)) are shown in figure 6. Figure 7 shows the relative density - time curves for the three mixtures in the remaining period (2-hr hold at 1700° C (3090° F)) of their pressure sintering runs. Light microscope examination made of the three pressure-sintered samples held at 1700° C (3090° F) showed a pore-free microstructure for all three. As previously mentioned for the pressure-sintered 100-percent-Si_3N_4 and 100-percent Al_2O_3 runs, measured density ρ_m values

(table I) for these three pressure-sintered samples were used in calculating relative densities, based upon light microscope examination of the samples showing them to be pore free.

It might be expected that the major densification in hot pressuring SiAlON-forming powder mixtures would occur during the holding period at the 1700° C (3090° F) and above temperatures which have been used. However, we found that the major amount of densification in all three mixtures (fig. 6) took place during the heating period. More significantly, on all three curves shown in figure 6, 90 percent or more of the total amount of densification (final density minus the initial as-cold-pressed density) was accomplished in the temperature range 1400° to 1700° C (2550° to 3090° F), which constitutes the last 30 minutes of the heating period. This 30-minute time span was obtained from figure 4 by noting the time difference between 1400° and 1700° C (2550° and 3090° F) on the heating schedule curve. The 2-hour hold at 1700° C (3090° F) following the heating period resulted in a density increase of only 2 percent or less of the final density, from a relative density of 98 to 100 percent, in the two lower-Al_2O_3-content samples and no increase in the third sample. Therefore, it is clear that at temperatures of 1700° C (3090° F) or higher, it is not necessary to employ a hold time for 1 to 2 hours in pressure sintering to produce dense SiAlON bodies, as has been the practice in the field.

A closer examination of the relative density - temperature curves in figure 6 reveals that, as the Al_2O_3 content in the sample increases, the curve more closely resembles the 100-percent-Al_2O_3 curve. On the $80Si_3N_4$-$20Al_2O_3$ curve, the sample essentially does not densify until the temperature reaches 1450° C (2640° F), above which temperature a high rate of densification occurs. On the $60Si_3N_4$-$40Al_2O_3$ curve, an initial rise in relative density occurs, beginning at about 1000° C (1830° F) and ending at about 1250° C (2280° F). This initial density rise is followed by an arrest in the temperature range 1250° to 1400° C (2280° to 2550° F) before the fast rise in relative density begins. On the $40Si_3N_4$-$60Al_2O_3$ curve, the initial rise in relative density begins at 1000° C (1830° F) and is followed by an arrest from 1200° (2190° F) to about 1300° C (2370° F) before the major increase in density begins. As for the 100-percent-Al_2O_3 curve, the initial rise in relative density between about 900° and 1200° C (1650° and 2190° F) is followed by an arrest before another rise in density begins at about 1350° C (2460° F).

The pressure-sintered Si_3N_4-Al_2O_3 samples which have been discussed were initially mechanical mixtures of Si_3N_4 particles and Al_2O_3 particles before interaction occurred between them. It is reasonable to assume that in a mechanical mixture of different powders the contribution of each powder constituent to the way the mixture compacts is related to the volume percentage of each particular powder constituent present in the mixture. As stated previously, we observed that as the amount of Al_2O_3 powder

in the Si_3N_4-Al_2O_3 powder mixtures increased, the resultant relative density - transient temperature curves (fig. 6) became more similar in form to the 100-percent-Al_2O_3 curve. Initially, the characteristic features of Al_2O_3 powder compaction were only slightly reflected in the 80-mol %-Si_3N_4 - 20-mol %-Al_2O_3 mixture, which contained 12.3-vol % Al_2O_3 (table I). However, the occurrence of enhanced densification in the $80Si_3N_4$-$20Al_2O_3$ mixture in comparison to 100-percent Al_2O_3 and 100-percent Si_3N_4 is evident beginning at 1400° C (2550° F) (fig. 6). At this temperature there is a fast and sustained rise in the relative density - transient temperature curve for the $80Si_3N_4$-$20Al_2O_3$ material. As the volume percentage of Al_2O_3 increases to 41.8 percent in the $40Si_3N_4$-$60Al_2O_3$ mixture (table I), the Al_2O_3 particles, being much finer both before and after stirred-ball-mill mixing with the coarser Si_3N_4 (fig. 2), are able to surround the larger Si_3N_4 particles. This explains why the characteristic compaction behavior of Al_2O_3 is clearly seen for the $40Si_3N_4$-$60Al_2O_3$ material. This material in the 1300° to 1700° C (2370° to 3090° F) temperature range also has a greater relative density than the 100-percent-Al_2O_3 sample - again indicating the enhanced densification. X-ray analysis results (discussed in the next section) shed more light on the type of reactions taking place in each temperature range during pressure sintering.

Densification at Holding Temperatures Below 1700° C

It has been stated in the preceding discussion that it might not be necessary to employ temperatures as high as 1700° C (3090° F) to produce dense SiAlON bodies by pressure sintering and also that a very active densification mechanism begins to operate in the temperature range 1350° to 1700° C (2460° to 3090° F). Therefore, in an attempt to provide more information regarding the compaction behavior of Si_3N_4-Al_2O_3 powder mixtures at temperatures below 1700° C (3090° F), a series of pressure sintering experiments with lower holding temperatures were made on samples with $40Si_3N_4$-$60Al_2O_3$ composition. In each such pressure sintering run, the heating schedule shown in figure 4 was followed to the desired holding temperature and then a 2-hour hold at that temperature was made.

The transient relative density of the sample throughout the entire pressure sintering run was calculated for each experiment following the procedures outlined in equations (1) to (4). For each lower-temperature pressure sintering run, the relative density - temperature data in the heating period closely reproduced the $40Si_3N_4$-$60Al_2O_3$ curve in figure 6 up to the desired holding temperature level. During the subsequent 2-hour holding period the sample might or might not increase its relative density depending on the level of the holding temperature. For a particular holding temperature, the relative density of a sample at the end of a 2-hour holding period minus its relative

density at the onset of the 2-hour hold is termed the "net change in relative density" during that 2-hour period. In figure 8, the net change in relative density of a sample is plotted against the corresponding holding temperature. A strong time- and temperature-dependent densification mechanism is clearly operative from approximately 1350° to 1700° C (2460° to 3090° F). Below this temperature range, the sample essentially did not increase its density during a 2-hour hold. Here a less time-dependent mechanism caused the sample to densify to a certain amount depending on temperature alone. From light microscope examination, samples with holding temperatures of 1500° C (2730° F) and higher were essentially pore free. Thus, the "net change in relative density" was slight at holding temperatures above 1550° C (2820° F) because the sample had attained a high relative density during the heating period. And so the possibility of further densification in the holding period was negligible. This is why at 1700° C (3090° F) the net change in relative density was zero. The high mobility in the Si_3N_4-Al_2O_3 system above about 1350° C (2460° F) suggests its utilization for mechanical forming such as forging and extrusion.

X-Ray Diffraction Analysis

The relative density results presented in the preceding sections indicate that densification of a sample in the temperature range 1350° to 1700° C (2460° to 3090° F) possibly involves one or more time- and temperature-dependent (thermally activicated) phenomena, such as diffusion, solutioning, and phase transformation. One effective method to reveal this information is X-ray diffraction. Experimental limitations prohibited direct X-ray examination of the sample during the pressure sintering experiments. In this study, all X-ray diffraction examinations were made on samples at room temperature after the pressure sintering run was completed. Helium gas was used to quench the sample at the end of pressure sintering to prevent further reaction taking place in the sample. Relative X-ray peak intensities were used to indicate the change in the relative amount of the phases present in the sample. The expansion in lattice parameters of a phase is interpreted as solid-solution formation.

X-ray results from samples of $40Si_3N_4$-$60Al_2O_3$ that had been pressure sintered at different holding temperatures (2-hr hold) are summarized in figure 9. Since we are interested only in the trend of the change in the relative amount of each phase present in the sample, a semiquantitative approach was used in presenting the relative density data. The $40Si_3N_4$-$60Al_2O_3$ composition is nearly 50 wt % Al_2O_3 and 50 wt % Si_3N_4 (table I). It is therefore a reasonable approximation to assign 0.5 as the reference relative X-ray peak intensity for Al_2O_3 and also for Si_3N_4 in the starting powder mixture before any reaction between Al_2O_3 and Si_3N_4 occurs. According to the suppliers,

Al_2O_3 powders are predominantly γ-Al_2O_3, while Si_3N_4 powders are composed of 94-percent α-Si_3N_4 and 6-percent β-Si_3N_4. Thus, the 0.5 relative X-ray peak intensity value assigned for Si_3N_4 is divided into 0.47 for α-Si_3N_4 and 0.03 for β-Si_3N_4.

In figure 9 the relative X-ray peak intensity of each phase present in the sample at the end of a pressure sintering experiment is plotted against the corresponding holding temperature. Reference relative X-ray peak intensity values of 0.5, 0.47, and 0.03 were used for γ-Al_2O_3, α-Si_3N_4, and β-Si_3N_4, respectively. Data from the two lowest-temperature pressure sintering runs (1200° and 1300° C; 2190° and 2370° F) showed no interaction between Si_3N_4 and Al_2O_3. The relative amounts of α-Si_3N_4 and β-Si_3N_4 remained unchanged, but almost all γ-Al_2O_3 had transformed to α-Al_2O_3 at 1200° C (2190° F) and no γ-Al_2O_3 was detectable at 1300° C (2370° F). (The plotted variation in the relative X-ray peak intensities for γ-Al_2O_3 and α-Al_2O_3 between 750° and 1200° C (1380° and 2190° F) shown in figure 9 is based on the reported temperature range for γ-Al_2O_3 to α-Al_2O_3 transformation (ref. 17).) Between 1300° and 1450° C (2370° and 2640° F), where α-Al_2O_3 and α-Si_3N_4 are the major phases and β-Si_3N_4 is present first as a trace amount, mutual solid solutioning between Si_3N_4 and Al_2O_3 is taking place. This is indicated by the double lines in figure 9. The β-Si_3N_4 phase begins to increase above 1300° C (2370° F) with the double lines denoting solutioning of Al_2O_3 in Si_3N_4 and formation of an expanded β-Si_3N_4 crystal structure termed β' (beta prime) by Jack and Wilson (ref. 9). The increase in the β' phase starting above approximately 1300° C (2370° F) corresponds to a resumption of densification, as was noted for $40Si_3N_4$-$60Al_2O_3$ in figure 6.

As shown in figure 9, at 1550° C (2820° F) a trace amount of a phase hereinafter referred to as X-phase was found. This phase was first found by Oyama and Kamigaito in hot-pressed Si_3N_4-Al_2O_3 powder compacts and is characterized as to interplanar spacings and relative intensities in reference 21. In subsequent work on Si_3N_4-Al_2O_3-Ga_2O_3 solid solutions (refs. 22 and 23), Oyama found this phase again and referred to it as X-phase. In the work reported herein, the X-phase increased in relative amount as the pressure sintering temperature increased to 1700° C (3090° F), the maximum temperature used in this study. X-phase may enhance the densification process by liquid-phase sintering. Drew and Lewis (ref. 11) present evidence for X-phase having been a liquid in sintering and hot-pressing studies to 1800° C (3270° F). And, indeed, our metallographic results (discussed in the next section) also give evidence for the presence of a liquid phase. Drew and Lewis (ref. 11) found that qualitatively the amount of surface SiO_2 associated with the α-Si_3N_4 powder determines the amount of X-phase formed. Previously, Oyama and Kamigaito (ref. 21) had found that additions of SiO_2 to a Si_3N_4-Al_2O_3 powder mix which was subsequently hot pressed resulted in an increased quantity of X-phase. In our studies, X-ray examinations were also made on $80Si_3N_4$-$20Al_2O_3$ and $60Si_3N_4$-$40Al_2O_3$ samples which had been pressure sintered at 1700° C

(3090° F) for 2 hours. The results, in comparison with the X-ray results from the $40Si_3N_4$-$60Al_2O_3$ sample already discussed, show that the relative amount of X-phase increases with increasing Al_2O_3 content. Such a relation between Al_2O_3 and X-phase in hot-pressed Si_3N_4-Al_2O_3 compositions is reported by Oyama and Kamigaito (ref. 21). We did not detect α-Si_3N_4 or α-Al_2O_3 at 1650° or 1700° C (3000° or 3090° F), with only β', the major phase, and X-phase being found in the samples.

Metallographic Examination

Light microscope examination of samples of Si_3N_4-Al_2O_3 compositions (in mol %) of 80-20, 60-40, and 40-60 which had been pressure sintered at 1700° C (3090° F) and 27.6 MN/m^2 (4000 psi) for 2 hours showed pore-free structures for all three. Figure 10 shows the $40Si_3N_4$-$60Al_2O_3$ microstructure, which is made up of a gray-matrix major phase, a darker uniformly dispersed minor phase, and a small amount of a bright, fine particle phase. The bright phase was identified as iron by scanning electron microscope (SEM) energy dispersion X-ray analysis. As mentioned previously, a small amount of iron, 0.4 to 0.8 wt %, was picked up from the steel grinding medium during the stirred-ball-mill blending of the Si_3N_4-Al_2O_3 powder mixtures. The darker minor phase in figure 10 was most prevalent for this highest-Al_2O_3-content sample and is believed to be the X-phase. The quantity of the darker minor phase was least in the $80Si_3N_4$-$20Al_2O_3$ microstructure and somewhat greater in the $60Si_3N_4$-$40Al_2O_3$ sample. These observations correlate with the X-ray results that indicated higher X-phase contents for higher Al_2O_3 levels. The gray-matrix major phase in figure 10 is the β' matrix.

More detailed microstructures of the three pressure-sintered compositions of Si_3N_4-Al_2O_3 (80-20, 60-40, and 40-60 mol %) were revealed by the transmission electron microscope (TEM) technique, as shown in figure 11. The three compositions at the same magnification (27 000) are shown in figure 11(a). Some of the rod-shaped Si_3N_4 grains which made up part of the Si_3N_4 powder morphology can be seen in figures 11(a-1) and (b-1) for the lowest Al_2O_3 concentration. At the higher Al_2O_3 levels (figs. 11(a-2) and (a-3)) no such grains are found. The grain size increased with Al_2O_3 content, and the overall grain morphology is equiaxed with predominantly faceted grain boundaries. Even in the sample with the highest Al_2O_3 content, there is no indication of retention of the original spherical particle morphology of the Al_2O_3. A striking feature in figure 11 is the striations in some grains (figs. 11(a-3) and (b-2), in particular). These grains generally have a rounded boundary, suggesting the presence of liquid at one time. The number of striated grains increases with increasing Al_2O_3 content. Grains with striations have been identified as X-phase by Drew and Lewis

(ref. 11) through transmission electron diffraction. The striations were interpreted by Drew and Lewis as twin and antiphase boundaries "believed to form as growth accidents either on solidification of the residual liquid of X-phase composition or via an order-disorder transformation during post solidification cooling" (ref. 11).

The drastic difference in particle morphology and size between the as-mixed powders and the pressure-sintered samples would suggest that active recrystallization and growth occurred during pressure sintering, probably resulting from a combination of solid-state diffusion and solid/liquid interaction (solution reprecipitation) phenomena. Jack and Wilson (ref. 9) proposed that solid-state diffusion in the Si_3N_4-Al_2O_3 system was enhanced by the increased vacancy concentration that resulted from the solutioning of Al_2O_3 (Al and O ions) into the Si_3N_4 lattice in β' solid-solution formation. Thus, the diffusion rate in the material increases with the Al_2O_3 concentration. This solid-solutioning phenomenon occurs at temperatures above 1300° C (2370° F), as shown in the X-ray results in the section X-Ray Diffraction Analysis. The solid/liquid interaction was postulated by several workers and has recently been more convicingly demonstrated by Drew and Lewis (ref. 11). As pointed out earlier, the amount of X-phase, the liquid phase at high temperature, increases with the Al_2O_3 content in the sample. Therefore, in accordance with these two proposed phenomena (models), it is easy to understand why the average grain size in samples (fig. 11) that have been pressure sintered under identical conditions increases with the Al_2O_3 content in the sample.

The Question of Oxygen and SiO_2 Contents

In our discussion of X-ray results the effect of SiO_2 on the quantity of X-phase formed was acknowledged by reference to the work of Drew and Lewis (ref. 11) and Oyama and Kamigaito (ref. 21). And Lange (ref. 13) has indicated that the effect of SiO_2 on the solutioning of Al_2O_3 in Si_3N_4 warrants further investigation. Since it is generally felt that the most desirable SiAlON material would be one free of second phases such as X-phase, the following information regarding the SiO_2 content of our materials is provided.

The oxygen content of the as-received Plessey α-Si_3N_4 was found by inert gas fusion to be 0.92 wt %. It has been postulated that oxygen stabilizes the α-Si_3N_4 structure when there is a minimum oxygen level of 0.90 wt %. A more likely oxygen level is 1.48 wt % (ref. 24). However, more recently, α-Si_3N_4 prepared by chemical vapor deposition was found to have an oxygen content of only 0.30 wt % (ref. 25). It has not been established just what minimum oxygen content in α-Si_3N_4 can be achieved through atmosphere control during production of Si_3N_4. Assuming the Plessey α-Si_3N_4 to have at least 0.30-wt % oxygen in solution would leave 0.62-wt % oxygen present in SiO_2. This

amount of SiO_2 was calculated to be 1.16 wt %, or 1.68 vol %. Oxygen pickup due to the 2-hour, stirred-ball-mill blending of the Si_3N_4-Al_2O_3 compositions was estimated at 2.49, 2.10, and 1.65 wt %, respectively, for the 80-20, 60-40, and 40-60 mol % Si_3N_4-Al_2O_3 compositions. These estimates were based on an oxygen analysis by inert gas fusion on a 100-percent-Si_3N_4 powder batch that was mixed in the same manner as the Si_3N_4-Al_2O_3 compositions. This oxygen pickup is believed to reflect oxidation of Si_3N_4 and the formation of an SiO_2 skin on the fine Si_3N_4 particles. The oxygen pickups correspond to SiO_2 volume percentages of 6.64, 5.59, and 4.42. Adding these values to the calculated amount of SiO_2 in the starting Si_3N_4 powder (assuming partitioning of the oxygen as discussed) then gives SiO_2 volume percentages of 8.32, 7.27, and 6.10, respectively, for the 80-20, 60-40, and 40-60 mol % Si_3N_4-Al_2O_3 compositions. Based on these percentages, it might be reasoned that the highest-SiO_2-content mixture, $80Si_3N_4$-$20Al_2O_3$ would have the most X-phase after pressure sintering. However, this was not the case; this pressure-sintered composition had the least X-phase. This indicates an Al_2O_3 concentration dependence, as we noted and which was formerly found by Oyama and Kamigaito (ref. 21). It is apparent that the control, or hopefully the elimination of X-phase in SiAlON, requires further work.

CONCLUDING REMARKS

In this experimental study of the Si_3N_4-Al_2O_3 (SiAlON) powder compacts under pressure-sintering conditions, a better understanding of the densification phenomenon was obtained by characterizing the solutioning and phase transformation phenomena in the material system and the microstructure of the pressure-sintered specimens. The new information generated can be used as a guide to better processing procedures for fabricating dense SiAlON bodies with controlled microstructures. The important findings from this study can be summarized as follows:

1. The densification behavior of Al_2O_3-Si_3N_4 powder compacts is dependent upon the solutioning and phase transformation phenomena in the material system. Solutioning and phase transformation were found to be very active in the temperature range 1400° to 1700° C (2550° to 3090° F), with a maximum at 1500° C (2730° F).

2. Fully dense bodies can be obtained at temperatures as low as 1500° C (2730° F) at 27.6 MN/m^2 (4000 psi) for 2 hours with no X-ray indication of X-phase. The lower hot-pressing temperature is more economical and the resulting microstructure (with a minimum amount of second phase) is potentially a better material.

3. A 100-percent-dense body can be obtained by heating to 1700° C (3090° F) at 27.6 MN/m^2 (4000 psi) without a holding time. The grain size of the dense body so produced should be much finer and therefore have higher mechanical strength than one pro-

duced by holding at 1700° C (3090° F) under pressure for 1 to 2 hours.

4. Because of the high mobility of the material system in the temperature range ~1350° to 1700° C (~2460° to 3090° F) (high rate of solutioning and phase transformation), it may be possible in this temperature range to mechanically form (similar to forging, extrusion, etc.) a dense SiAlON body into a desired shape.

5. New pressureless sintering procedures could also be based on the results of this study.

SUMMARY OF RESULTS

In this investigation, a pressure-sintering technique was employed to investigate solution formation and densification mechanisms of blends of silicon nitride (Si_3N_4) and aluminum oxide (Al_2O_3) powders. Four aspects of the problem were examined: (1) the effect of Si_3N_4:Al_2O_3 mole ratio on densification behavior, (2) the variation of the relative density of the powder compact with temperature and time during pressure sintering, (3) X-ray phase analysis of bodies that had been pressure sintered at 27.6 MN/m^2 (4000 psi) and various temperatures for 2 hours, and (4) metallographic analysis of the pressure-sintered bodies.

It is well to qualify this summary by restating that our Si_3N_4-Al_2O_3 mixtures that were converted to SiAlON bodies by pressure sintering did contain considerable amounts of silicon dioxide (SiO_2) (calculated based on oxygen analyses). For example, 6.10-mol % SiO_2 was found in the 40-mol %-Si_3N_4 - 60-mol % Al_2O_3 mixture. Silicon dioxide is thought to influence the densification behavior of SiAlON.

The results from these experimental studies are summarized as follows:

1. Essentially pore-free SiAlON bodies were obtained for all three blends (mole ratios of 4:1, 3:2, and 2:3) of Si_3N_4 and Al_2O_3 powders after pressure sintering at 27.6 MN/m^2 (4000 psi) and 1700° C (3090° F) for 2 hours. These dense bodies consist of mainly β' (SiAlON) solid solution with a minor amount of a particular second phase, termed X-phase, first found by Oyama and Kamigaito. Under the same pressure-sintering conditions, Si_3N_4 powder virtually did not compact, and Al_2O_3 powder densified to only 88 percent of theoretical density.

2. The higher the Al_2O_3 content in a SiAlON in the range 20 to 50 mol %, the higher was the densification rate and the more nearly it reflected the characteristic densification behavior of Al_2O_3.

3. Metallographic results showed that

   a. No spherical grains typical of the Al_2O_3 starting powder remained after any SiAlON formation, regardless of Al_2O_3 content, thus indicating complete Al_2O_3 solutioning.

b. Rod-shaped Si_3N_4 grains, which made up part of the starting Si_3N_4 powder morphology, could still be seen in the 20-mol %-Al_2O_3 SiAlON. But at higher Al_2O_3 contents, these rod-shaped Si_3N_4 grains had recrystallized by solutioning and phase transformation.

c. As the Al_2O_3 content of the SiAlON was increased, the equiaxed grain size increased and the amount of X-phase (apparently once liquid) increased. It is suggested that grain growth resulted from a solution-precipitation model (as proposed by Drew and Lewis) and from vacancy promoted diffusion (as proposed by Jack).

4. For the 60-mol %-Al_2O_3 SiAlON, which was selected for more extensive study, it was found

a. That densification to 1300° C (2370° F) was due to the characteristic compaction behavior of Al_2O_3, involving particle sliding

b. That densification above 1400° C (2550° F) also reflected Al_2O_3 compaction behavior but was hastened and sustained by mutual solutioning between Si_3N_4 and Al_2O_3 and the formation of β'

c. That densification above 1500° C (2730° F) was aided by the formation of a liquid phase (X-phase) with solid/liquid interaction

Lewis Research Center,
National Aeronautics and Space Administration,
Cleveland, Ohio, July 9, 1975,
505-01.

REFERENCES

1. McLean, A. F.; Fisher, E. A.; and Harrison, D. E.: Brittle Materials Design, High Temperature Gas Turbine. Ford Motor Co. (AMMRC-CTR-72-3; AD-894052), 1972.

2. McLean, A. F.; Fisher, E. A.; and Harrison, D. E.: Brittle Materials Design, High Temperature Gas Turbine. Ford Motor Co. (AMMRC-CTR-72-19; AD-905043), 1972.

3. McLean, A. F.; Fisher, E. A.; and Bratton, R. J.: Brittle Materials Design, High Temperature Gas Turbine. Ford Motor Co. (AMMRC-CTR-73-9; AD-910446), 1973.

4. McLean, A. F.; Fisher, E. A.; and Bratton, R. J.: Brittle Materials Design, High Temperature Gas Turbine. Ford Motor Co. (AMMRC-CTR-73-32; AD-914451), 1973.

5. McLean, A. F.; Fisher, E. A.; and Bratton, R. J.: Brittle Materials Design, High Temperature Gas Turbine. Ford Motor Co. (AMMRC-CTR-74-26; AD-920691), 1974.

6. McLean, A. F.; Fisher, E. A.; and Bratton, R. J.: Brittle Materials Design, High Temperature Gas Turbine. Ford Motor Co. (AMMRC-CTR-74-59), 1974.

7. Lange, F. F.: Strong High Temperature Ceramics. Ann. Rev. Mater. Sci., vol. 4, 1974, pp. 365-390.

8. Torti, M. L.: Ceramics for Gas Turbines - Present and Future. SAE Paper 740242, Feb. 1974.

9. Jack, K. H.; and Wilson, W. I.: Ceramics Based on the Si-Al-O-N and Related Systems. Nature Phys. Sci., vol. 238, no. 7, July 1972, pp. 28-29.

10. Jack, K. H.: Nitrogen Ceramics. British Ceramic Soc. Trans. and J., vol. 72, no. 8, Aug. 1973, pp. 376-384.

11. Drew, P.; and Lewis, M. H.: The Microstructures of Silicon Nitride/Alumina Ceramics. J. Mat. Sci., vol. 9, 1974, pp. 1833-1838.

12. Arrol, W. J.: The Sialons-Properties and Fabrication. Chapt. 34 in Ceramics for High-Performance Applications. Proc. 2nd Army Materials Technology Conf., Brook Hill Publ. Co., 1974, pp. 729-738.

13. Lange, F. F.: Fabrication and Properties of Silicon Compounds - Task I. Fabrication Microstructure and Selected Properties of SiAlON Compositions. Westinghouse Research Labs., Feb. 1974.

14. Crandall, W. B.; Hed, A. Z.; and Shipley, L. E.: Preparation and Evaluation of SiAlON. Final Report ARL-TR-74-0099 Aerospace Res. Labs., Air Force Systems Command, June 1974.

15. Terwilliger, G. R.; and Lange, F. F.: Hot-Pressing Behavior of Si_3N_4. J. American Ceram. Soc., vol. 57, no. 1, Jan. 1974, pp. 25-29.

16. Rossi, Ronald C.; and Fulrath, Richard M.: Final Stage Densification in Vacuum Hot-Pressing of Alumina. J. American Ceram. Soc., vol. 48, no. 11, Nov. 1965, pp. 558-564.

17. Lynch, James F.; Ruderer, Clifford G.; and Duckworth, Winston H.: Engineering Properties of Ceramics - Databook to Guide Materials Selection for Structural Application. Battelle Memorial Inst. (AFML-TR-66-52; AD-803765), 1966.

18. Rice, Roy W.: Fabrication and Characterization of Hot-Pressed Al_2O_3. NRL-7111, Naval Research Lab. (AD-709556), 1970.

19. Gazza, G. E.; Barfield, J. R.; and Preas, D. L.: Reactive Hot-Pressing of Alumina with Additives. American Ceram. Soc. Bull., vol. 48, no. 6, June 1969, pp. 606-610.

20. Rice, R.: Hot Forming of Ceramics. Chapter 11 in Ultrafine-Grain Ceramics, Proc. 15th Sagamore Army Materials Research Conf., Syracuse University Press, 1970, pp. 203-250.

21. Oyama, Y.; and Kamigaito, O.: Hot-Pressing of Si_3N_4-Al_2O_3. J. Ceram. Soc. Japan., vol. 80, No. 8, 1972, pp. 327-336.

22. Oyama, Y.: Solid Solution in the Ternary System, Silicon Nitride - Aluminum Oxide - Gallium Oxide. Jap. J. Appl. Phys., vol. 11. no. 10, Oct. 1972, p. 1572.

23. Oyama, Y.: Solid Solution in the System Silicon Nitride - Gallium Oxide - Aluminum Oxide. Jap. J. Appl. Phys., vol. 12, no. 4, Apr. 1973, pp. 500-508.

24. Wild, S.; Grieveson, P.; and Jack, K. H.: The Crystal Structures of Alpha and Beta Silicon and Germanium Nitrides. Chapter 28 in Special Ceramics 5, P. Popper, ed., British Ceramic Research Assoc., Stoke-On-Trent, England, 1972, pp. 385-395.

25. Priest, H. F.; Burns, F. C.; Priest, G. L.; and Skarr, E. C.: Oxygen Content of Alpha Silicon Nitride. J. American Ceram. Soc., vol. 56, no. 7, July 1973, p. 395.

TABLE I. - COMPOSITIONS AND DENSITIES OF

PRESSURE-SINTERED Si_3N_4-Al_2O_3

Si_3N_4:Al_2O_3 mole ratio	Al_2O_3 content			Density of compacts pressure sintered at 1700° C (3090° F) and 27.6 MN/m^2 (4000 psi) for 2 hr		
	mol %	wt %	vol %	Measured (immersion) density, ρ_m, g/cm^3	Density of perfect mechanical mixture, g/cm^3	Density of complete solid (β') solution, g/cm^3
100-Percent Si_3N_4	0	0	0	[a]~1.6	----	----
4:1	20	15.4	12.3	3.23	3.29	3.12
3:2	40	32.6	26.1	3.15	3.41	3.08
2:3	60	52.2	41.8	3.10	3.56	3.00
100-Percent Al_2O_3	100	100	100	3.48	----	----

[a]Bulk density.

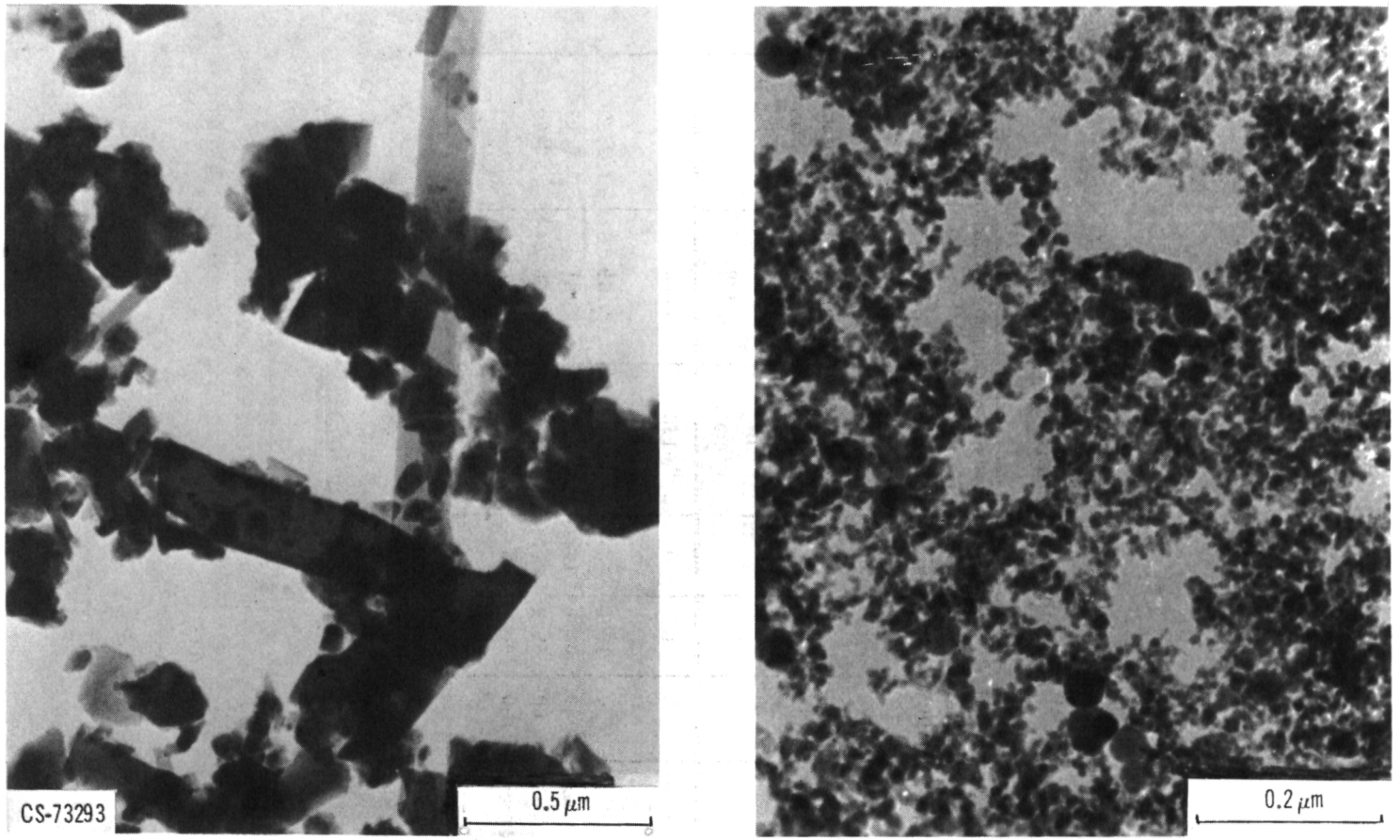

(a) α-Si_3N_4.

(b) γ-Al_2O_3.

Figure 1. - Transmission electron micrographs showing the as-received Si_3N_4 and Al_2O_3 powder morphologies and typical particle sizes.

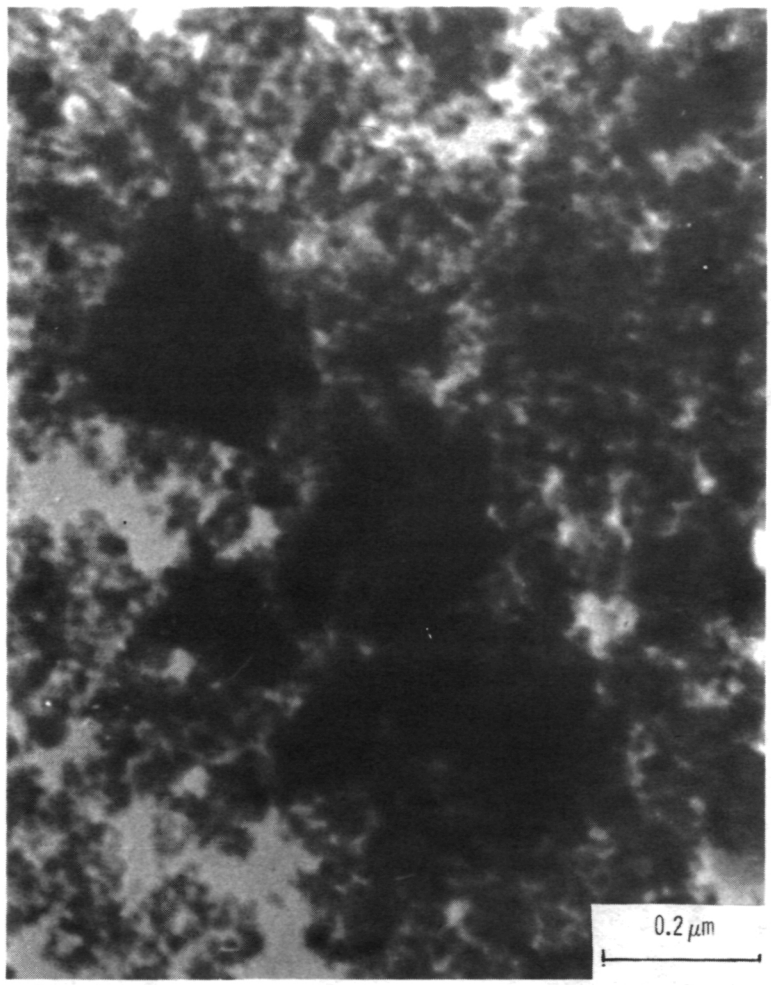

Figure 2. - Transmission electron micrograph showing $40Si_3N_4$-$60Al_2O_3$ powder mixture after stirred-ball-mill blending.

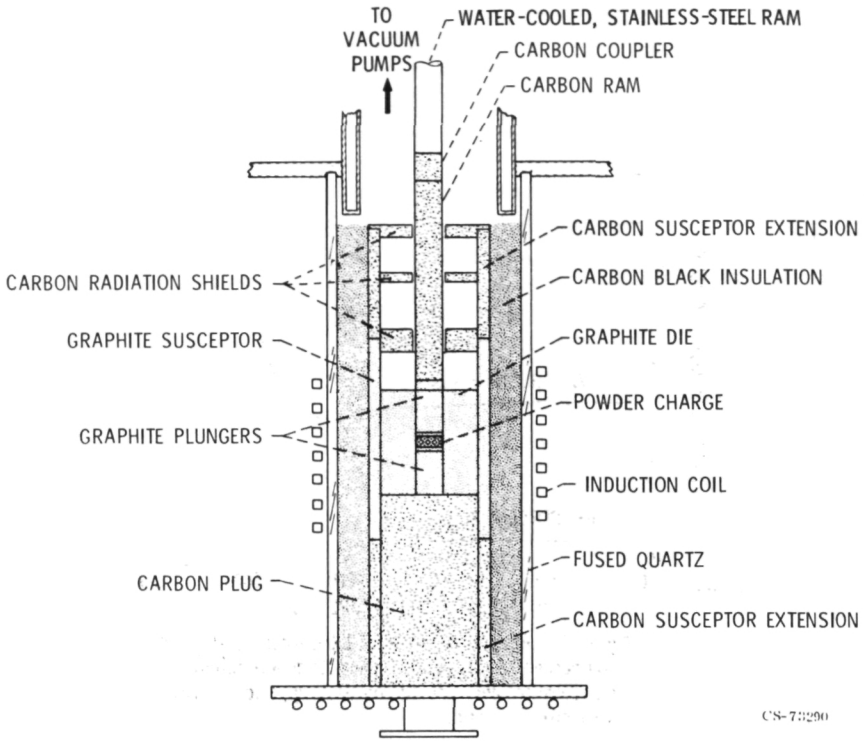

Figure 3. - Schematic of vacuum induction furnace used for pressure sintering.

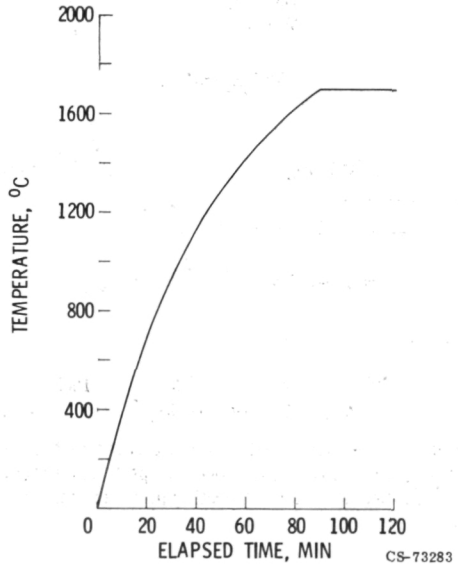

Figure 4. - Heating schedule of a typical pressure sintering run.

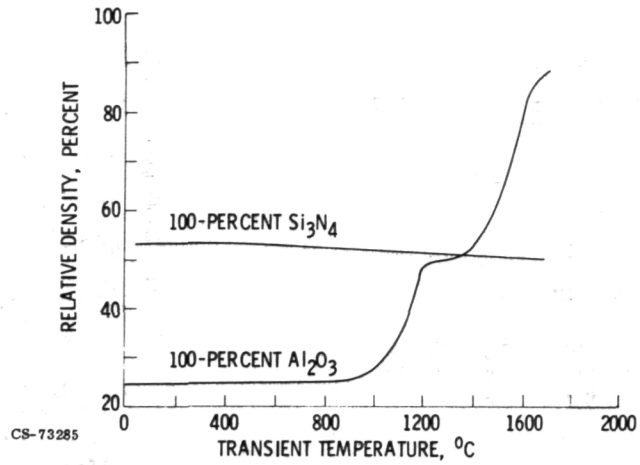

Figure 5. - Relative densities of 100-percent-Si_3N_4 and 100-percent-Al_2O_3 powder compacts as a function of transient temperature during heating period of pressure sintering run.

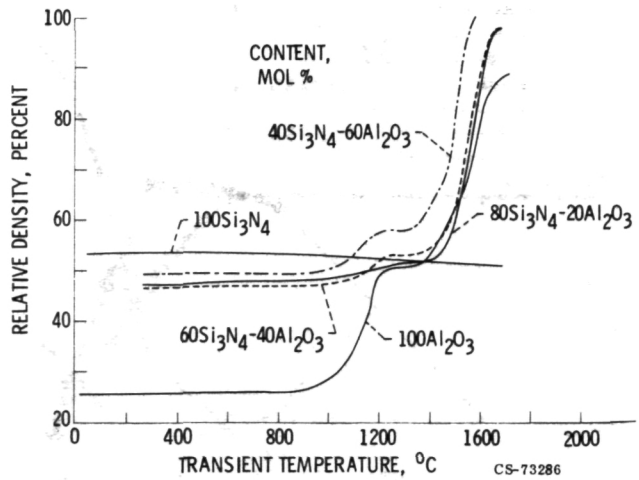

Figure 6. - Relative densities of 100-percent-Si_3N_4, 100-percent-Al_2O_3, and Si_3N_4-Al_2O_3 powder compacts as a function of transient temperature during heating period of pressure sintering run.

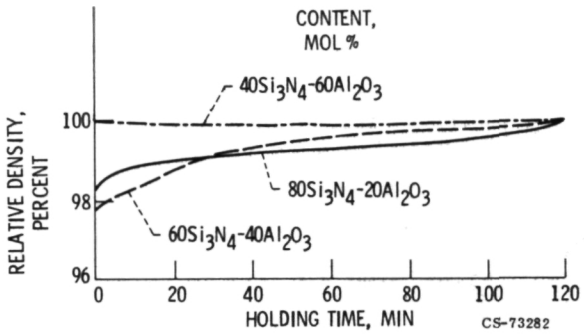

Figure 7. - Relative densities of Si_3N_4-Al_2O_3 powder compacts as a function of time held at 1700° C (3090° F) and 27.6 MN/m^2 (4000 psi).

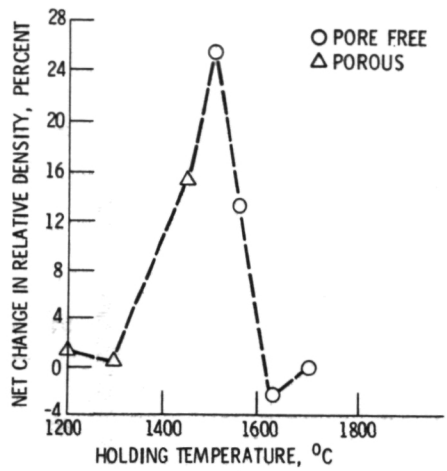

Figure 8. - Net change in relative densities of 40-mol %-Si_3N_4 - 60-mol %-Al_2O_3 powder compacts during 2-hour holding periods at temperatures to 1700° C (3090° F).

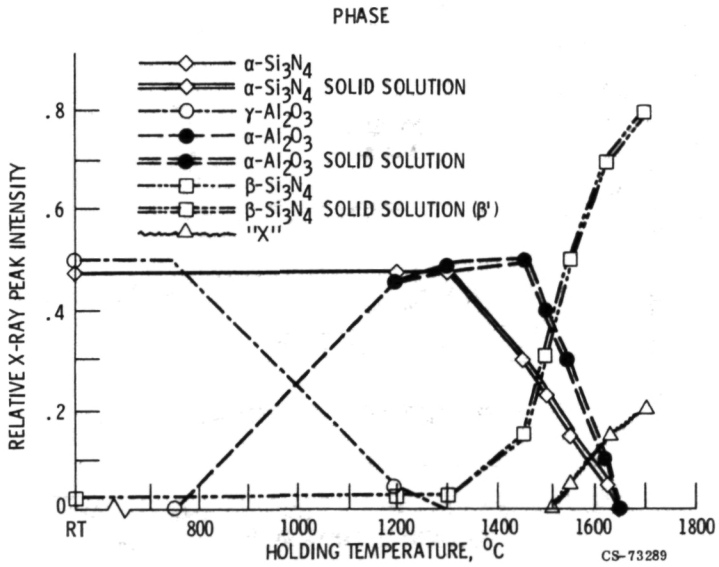

Figure 9. - Relative X-ray peak intensities for phases present in 40-mol %-Si_3N_4 - 60-mol %-Al_2O_3 powder compacts after pressure sintering followed by 2-hour holding period at temperature to 1700° C (3090° F).

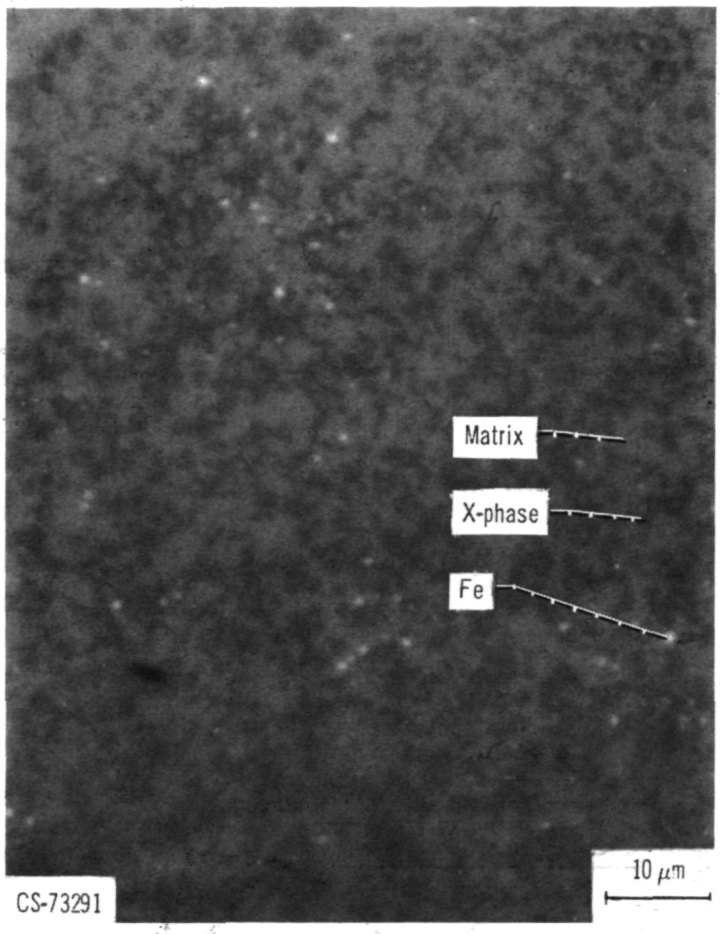

Figure 10. - Microstructure of $40Si_3N_4$-$60Al_2O_3$ powder compact after pressure sintering at 1700° C (3090° F) and 27.6 MN/m^2 (4000 psi) for 2 hours.

(a-1) $80Si_3N_4$-$20Al_2O_3$.

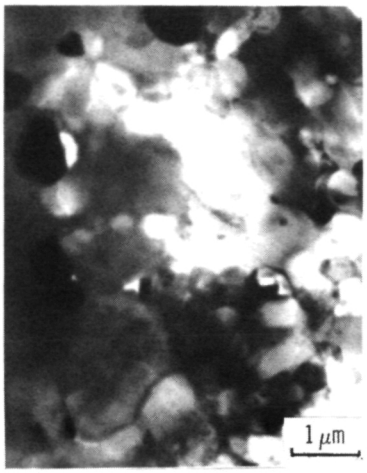

(a-2) $60Si_3N_4$-$40Al_2O_3$.

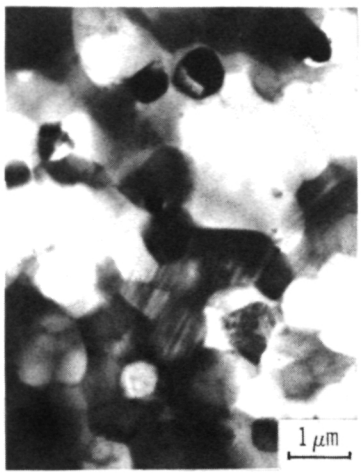

(a-3) $40Si_3N_4$-$60Al_2O_3$.

(a) Magnification, 27 000.

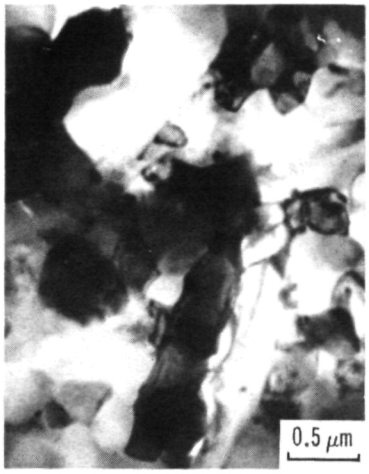

(b-1) $80Si_3N_4$-$20Al_2O_3$.

(b-2) $40Si_3N_4$-$60Al_2O_3$.

CS-73294

(b) Magnification, 54 000

Figure 11. - Transmission electron micrographs of Si_3N_4-Al_2O_3 powder compacts (in mol%) after pressure sintering at 1700° C (3090° F) and 27.6 MN/m^2 (4000 psi) for 2 hours.

"The aeronautical and space activities of the United States shall be conducted so as to contribute . . . to the expansion of human knowledge of phenomena in the atmosphere and space. The Administration shall provide for the widest practicable and appropriate dissemination of information concerning its activities and the results thereof."

—NATIONAL AERONAUTICS AND SPACE ACT OF 1958

NASA SCIENTIFIC AND TECHNICAL PUBLICATIONS

TECHNICAL REPORTS: Scientific and technical information considered important, complete, and a lasting contribution to existing knowledge.

TECHNICAL NOTES: Information less broad in scope but nevertheless of importance as a contribution to existing knowledge.

TECHNICAL MEMORANDUMS: Information receiving limited distribution because of preliminary data, security classification, or other reasons. Also includes conference proceedings with either limited or unlimited distribution.

CONTRACTOR REPORTS: Scientific and technical information generated under a NASA contract or grant and considered an important contribution to existing knowledge.

TECHNICAL TRANSLATIONS: Information published in a foreign language considered to merit NASA distribution in English.

SPECIAL PUBLICATIONS: Information derived from or of value to NASA activities. Publications include final reports of major projects, monographs, data compilations, handbooks, sourcebooks, and special bibliographies.

TECHNOLOGY UTILIZATION PUBLICATIONS: Information on technology used by NASA that may be of particular interest in commercial and other non-aerospace applications. Publications include Tech Briefs, Technology Utilization Reports and Technology Surveys.

Details on the availability of these publications may be obtained from:

SCIENTIFIC AND TECHNICAL INFORMATION OFFICE

NATIONAL AERONAUTICS AND SPACE ADMINISTRATION

Washington, D.C. 20546